

# Fluoro-Phenyl-Styrene-Sulfonamide, a Novel Inhibitor of $\sigma^B$ Activity, Prevents the Activation of $\sigma^B$ by Environmental and Energy Stresses in *Bacillus subtilis*

Daina L. Ringus,<sup>a</sup> Ahmed Gaballa,<sup>b</sup> John D. Helmann,<sup>b</sup> Martin Wiedmann,<sup>a</sup> Kathryn J. Boor<sup>a</sup>

Department of Food Science<sup>a</sup> and Department of Microbiology,<sup>b</sup> Cornell University, Ithaca, New York, USA

**Sigma B ( $\sigma^B$ ) is an alternative sigma factor that regulates the general stress response in *Bacillus subtilis* and in many other Gram-positive organisms.  $\sigma^B$  activity in *B. subtilis* is tightly regulated via at least three distinct pathways within a complex signal transduction cascade in response to a variety of stresses, including environmental stress, energy stress, and growth at high or low temperatures. We probed the ability of fluoro-phenyl-styrene-sulfonamide (FPSS), a small-molecule inhibitor of  $\sigma^B$  activity in *Listeria monocytogenes*, to inhibit  $\sigma^B$  activity in *B. subtilis* through perturbation of signal transduction cascades under various stress conditions. FPSS inhibited the activation of  $\sigma^B$  in response to multiple categories of stress known to induce  $\sigma^B$  activity in *B. subtilis*. Specifically, FPSS prevented the induction of  $\sigma^B$  activity in response to energy stress, including entry into stationary phase, phosphate limitation, and azide stress. FPSS also inhibited chill induction of  $\sigma^B$  activity in a  $\Delta rsbV$  strain, suggesting that FPSS does not exclusively target the RsbU and RsbP phosphatases or the anti-anti-sigma factor RsbV, all of which contribute to posttranslational regulation of  $\sigma^B$  activity. Genetic and biochemical experiments, including artificial induction of  $\sigma^B$ , analysis of the phosphorylation state of the anti-anti-sigma factor RsbV, and *in vitro* transcription assays, indicate that while FPSS does not bind directly to  $\sigma^B$  to inhibit activity, it appears to prevent the release of *B. subtilis*  $\sigma^B$  from its anti-sigma factor RsbW.**

**S**igma B ( $\sigma^B$ ), an alternative sigma factor that regulates the general stress response in *Bacillus subtilis*, is conserved in many Gram-positive bacteria, including the pathogens *Listeria monocytogenes*, *Staphylococcus aureus*, and *Bacillus anthracis* (1). In both *L. monocytogenes* (2, 3) and *B. subtilis* (4, 5), activation of  $\sigma^B$  leads to the rapid, coordinated induction of more than 100 genes that collectively enhance survival under changing and often harsh physiological conditions. In addition to its regulation of the general stress response,  $\sigma^B$  modulates the expression of virulence factors important for pathogenesis in *L. monocytogenes* (6, 7), *B. anthracis* (8), and *S. aureus* (9, 10). The importance of  $\sigma^B$  as a regulator of both the stress response and virulence factor expression suggests that this alternative sigma factor may serve as a potential target for therapeutic intervention strategies during infection by these pathogens.

Our group previously used high-throughput screening of small-molecule libraries to identify inhibitors of  $\sigma^B$  activity in *L. monocytogenes* (11). The goal of these efforts was to identify novel tools that would enable study of the complex signaling pathways used by Gram-positive organisms to respond to environmental changes, with the potential for devising more-effective strategies to control the virulence of this pathogen and related organisms. We identified fluoro-phenyl-styrene-sulfonamide (FPSS) as a novel inhibitor of  $\sigma^B$  activity in *L. monocytogenes* and showed that FPSS also inhibits  $\sigma^B$  activity in *B. subtilis* in response to an environmental stress, the presence of 0.3 M NaCl (11). However, the mode of FPSS action was not identified.

In the present study, we sought to determine the mechanism by which FPSS prevents  $\sigma^B$  activity. Because FPSS inhibits  $\sigma^B$  activity in both *L. monocytogenes* and *B. subtilis*, we hypothesized that the small molecule operates through similar mechanisms in these related organisms, which share highly conserved *sigB* operons (1). We chose to exploit the multiple  $\sigma^B$ -activating systems in *B. sub-*

*tilis* to conduct experiments with the goal of identifying the protein(s) with which FPSS interacts to inhibit  $\sigma^B$ .

The activity of  $\sigma^B$  is tightly regulated in *B. subtilis* by three distinct pathways that integrate responses to stress (reviewed in reference 12) (Fig. 1). One branch of the signal transduction cascade relays the response to environmental stresses (such as the presence of high levels of salt, acid, or ethanol) through a 1.8-MDa multiprotein stressosome complex comprising the RsbS antagonist, RsbR coantagonists, and the RsbT serine/threonine kinase (13–15). In stressed cells, RsbT phosphorylates the antagonist RsbS and the coantagonist RsbRA, allowing RsbT to be released from the stressosome, which activates the phosphatase RsbU (16–19). Active RsbU, in turn, dephosphorylates the anti-anti-sigma factor RsbV, allowing it to bind to the anti-sigma factor RsbW, thus promoting the release of  $\sigma^B$  from RsbW. In a second branch, activation of  $\sigma^B$  in response to energy stresses (such as limitation of glucose, ATP, GTP, or phosphate) requires RsbP and RsbQ (20–22). The phosphatase RsbP dephosphorylates RsbV-P (phosphorylated RsbV), again resulting in a partner switch and the release of  $\sigma^B$  from RsbW. Finally,  $\sigma^B$  activation occurs in response to growth at low temperatures independently of RsbT, RsbU, and RsbV, in a manner not fully understood (23).

In contrast, several lines of evidence indicate that the *L. monocytogenes*  $\sigma^B$  response to environmental and energy stresses occurs through a single pathway via the stressosome (24–26). For example, *L. monocytogenes* lacks genes encoding homologs of the *B.*

Received 28 January 2013 Accepted 20 March 2013

Published ahead of print 22 March 2013

Address correspondence to Kathryn J. Boor, kjb4@cornell.edu.

Copyright © 2013, American Society for Microbiology. All Rights Reserved.

doi:10.1128/JB.00107-13

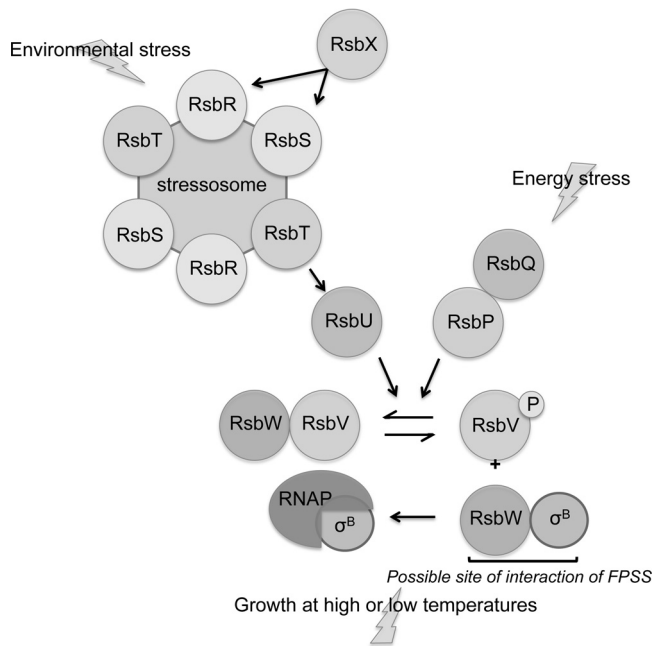


**FIG 1** Model of  $\sigma^B$  regulation in *B. subtilis*. The stressosome senses environmental stress signals and activates the positive regulator RsbU, which dephosphorylates RsbV-P. Unphosphorylated RsbV binds to RsbW, freeing  $\sigma^B$ . RsbQ and RsbP are required for  $\sigma^B$  activation in response to energy stress; RsbP dephosphorylates RsbV-P. Growth at high or low temperatures leads to  $\sigma^B$  activation independently of RsbV. References are cited in the text. The possible site of FPSS interaction is noted at the RsbW-SigB interface. (Modified from the *Annual Review of Microbiology* [12] with permission of the publisher.)

*subtilis* RsbP and RsbQ energy stress response pathway proteins (25, 26). Further, replacement of the four *B. subtilis* *rsbR* paralogs with *L. monocytogenes* *rsbR* within the *sigB* operon in *B. subtilis* allows for the activation of  $\sigma^B$  by energy stresses, suggesting that this *L. monocytogenes* paralog may integrate responses to both energy and environmental stresses (27). Finally, RsbU is necessary for  $\sigma^B$  activation in response to environmental and energy stresses (24–26), further supporting the single-pathway model of  $\sigma^B$  activation in *L. monocytogenes*.

We methodically investigated all known proteins involved in the signal transduction cascade that regulates *B. subtilis*  $\sigma^B$  in order to determine at which point FPSS disrupts  $\sigma^B$  activity. In particular, we explored the four shared components of the branches of the signal transduction pathway: the protein phosphatase domains of RsbU and RsbP, the components downstream of RsbV, the ability of  $\sigma^B$  to initiate transcription by association with RNA polymerase (RNAP), and the recognition of  $\sigma^B$  promoters by the sigma factor. Our experiments show (i) that FPSS appears to act independently and downstream of RsbV and (ii) that FPSS does not interact with  $\sigma^B$  *in vivo* or *in vitro*. Therefore, we conclude that FPSS interferes with a shared component of the two pathways, and the most likely target is the partner-switching mechanism involving  $\sigma^B$  and RsbW.

## MATERIALS AND METHODS

**Bacterial strains and genetic methods.** All strains used in this study are listed in Table 1. Strains PB2, PB198, PB206, PB213, and PB345 were provided by C. W. Price (University of California, Davis). Strains (renamed FSL B2-273 and FSL B2-274 for this study) for the overexpression of His<sub>6</sub>-SigB and His<sub>6</sub>-SigA were provided by W. Goebel (Universität Würzburg, Germany).

Strains expressing *B. subtilis* RsbV were constructed by cloning a PCR fragment containing *rsbV* amplified using primers DR34 and

**TABLE 1** Plasmids and strains used in this study

Plasmid or strain	Relevant genotype	Source
<b>Plasmids</b>		
pDLR1	<i>P<sub>fri Lm</sub> SigA2 SigB</i> in pUC19; Ap <sup>r</sup>	This study
pDLR2	<i>P<sub>spac</sub> rsbV<sub>Bs</sub></i> ; Neo <sup>r</sup>	This study
pCK35	<i>P<sub>spac</sub> Δ(rsbR rsbS) rsbT<sup>+</sup></i> ; Neo <sup>r</sup>	17
pUC19	High-copy-number cloning vector; Ap <sup>r</sup>	28
pQE-30	N-terminal His <sub>6</sub> expression vector; <i>P<sub>T7</sub>/O<sub>lac</sub></i> ; ColEI ori; Ap <sup>r</sup>	Qiagen
<b>Strains</b>		
<i>B. subtilis</i>		
FSL B2-303	<i>P<sub>spac</sub> rsbV<sub>Bs</sub> amyE::ctc-lacZ trpC2</i>	pDLR2→PB198
FSL B2-304	<i>P<sub>spac</sub> rsbV<sub>Bs</sub> amyE::ctc-lacZ trpC2 sigBΔ3::spc trpC2</i>	pDLR2→PB345
PB2	<i>trpC2</i>	29
PB198	<i>amyE::ctc-lacZ trpC2</i>	30
PB206	<i>rsbVΔ1 amyE::pDH32-ctc</i>	30
PB213	<i>P<sub>spac</sub> (rsbV<sup>+</sup> rsbWΔ1 sigB<sup>+</sup> rsbX<sup>+</sup>) amyE::pDH32-ctc trpC2</i>	30
PB345	<i>amyE::ctc-lacZ trpC2 sigBΔ3::spc trpC2</i>	31
<i>E. coli</i>		
FSL B2-273	M15 pREP4 pQE-30 His <sub>6</sub> -SigA <sub>Lm</sub>	32
FSL B2-274	M15 pREP4 pQE-30 His <sub>6</sub> -SigB <sub>Lm</sub>	32
FSL B2-302	TOP10 pUC19- <i>P<sub>fri Lm</sub></i>	pDLR1→TOP10
TOP10	F <sup>-</sup> <i>mcrA</i> Δ( <i>mrr-hsdRMS-mcrBC</i> ) φ80 <i>lacZ</i> ΔM15 Δ <i>lacX74 recA1 araD139</i> Δ( <i>ara-leu</i> )7697 <i>galU galK rpsL</i> (Str <sup>r</sup> ) <i>endA1 nupG</i>	Invitrogen
<i>L. monocytogenes</i>		
10403S	Wild type; serotype 1/2a	33
10403SΔ <i>sigB</i>	Δ <i>sigB</i>	34

TABLE 2 Primers and probes used in this study

Primer or probe	Sequence (5'→3') <sup>a</sup>	Source or reference
DR1 FRI Fwd	CGA <u>AGCTT</u> CACCTGAAAGCGGTGAGAAT	This study
DR2 FRI Rev	CTCTAG <u>ACCAGT</u> TGTGGA <u>AACCAT</u> CACA	This study
DR34 rsbV Fwd	GAT <u>AAGCTT</u> AAAGCAACTAGTGTATTGAAGGAAAA	This study
DR35 rsbV Rev	GATGCATGCCGGCACTTTTCATTTCGATGT	This study
<i>sigB</i> TaqMan F	GCCGCTTACCAAGAAAATGG	S. Chaturongakul, unpublished
<i>sigB</i> TaqMan R	TTCGGGCGATGGACTCTACT	S. Chaturongakul, unpublished
<i>sigB</i> MGB probe	ATCAAGACGCCCAATAT	S. Chaturongakul, unpublished
<i>rpoB</i> TaqMan F	CCGGACGTCACGGTAACAA	36
<i>rpoB</i> TaqMan R	CAGGTGTTCCGTCTGGCATA	36
<i>rpoB</i> MGB probe	CCGGACGTCACGGTAACAA	36

<sup>a</sup> Restriction sites are underlined.

DR35 (Table 2) into the pCK35 vector (17) at HindIII and SphI sites and confirming the presence of *rsbV* by sequencing at the Cornell University Life Sciences Core Laboratories Center. The resulting plasmid, pDLR2, was transformed by electroporation (35) into strains PB198 and PB345. For *in vitro* transcription assays, a 276-bp PCR fragment amplified using primers DR1 and DR2 (Table 2), which contain SigA2- and SigB-dependent promoter elements from the *L. monocytogenes fri* promoter region (37), was cloned into PUC19 at HindIII and XbaI sites and was transformed into *Escherichia coli* TOP10, resulting in strain FSL B2-302. Chloramphenicol (10 µg/ml), streptomycin (100 µg/ml), kanamycin (25 µg/ml), ampicillin (100 µg/ml), and neomycin (5 µg/ml) were added to media as appropriate.

**Overproduction and purification of  $\sigma^B$  and  $\sigma^A$  for *in vitro* transcription.** His<sub>6</sub>-SigB and His<sub>6</sub>-SigA proteins were overexpressed from strains FSL B2-273 and FSL B2-274. Cells were grown in 500 ml Luria broth (LB) containing ampicillin and kanamycin at 37°C with shaking (225 rpm). At an optical density at 600 nm (OD<sub>600</sub>) of 0.7 to 1.0, 1 mM isopropyl-β-D-thiogalactopyranoside (IPTG) was added. Cells were pelleted by centrifugation (10,000 × g, 15 min, 4°C) after 3 to 4 h of growth with IPTG and were frozen at -80°C. To purify proteins, cell pellets were thawed and resuspended in 5 ml lysis buffer (20 mM Tris [pH 8.0], 0.5 M NaCl, 5 mM imidazole, 6 M guanidine hydrochloride, 1 mM β-mercaptoethanol, 1 mg/ml lysozyme). Cells were sonicated (4 times, with 20 s on and 1 min off, at 33 W) on ice, and the lysate was centrifuged (10,000 × g, 15 min, 4°C) to remove cell debris. Supernatants were applied to a Ni-nitrilotriacetic acid (NTA) column (HisTrap HP; GE Life Sciences, Pittsburgh, PA) using a 10-ml syringe. On-column refolding was performed using a stepwise gradient of a buffer (20 mM Tris [pH 8.0], 0.5 M NaCl, 5 mM imidazole, 1 mM β-mercaptoethanol) containing decreasing concentrations of urea, according to the manufacturer's instructions. Following elution, protein fractions were analyzed using SDS-PAGE and Coomassie blue staining. Fractions containing target protein were concentrated (Vivaspin 2; molecular weight cutoff [MWCO], 10,000; GE Life Sciences), exchanged into protein storage buffer (10 mM Tris [pH 8.0], 10 mM MgCl<sub>2</sub>, 0.1 mM EDTA, 0.1 mM dithiothreitol [DTT], 0.1 M NaCl, 50% glycerol), and stored at -20°C.

**Growth conditions and β-galactosidase assays.** All *B. subtilis* strains were grown with shaking (225 rpm) in 300-ml Nephelo flasks (Bellco, Vineland, NJ). Strains PB213, FSL B2-303, and FSL B2-304 were grown in buffered LB (BLB) (31). For azide and salt stress experiments, strains grown overnight in LB at 37°C were diluted (1:25) into 30 ml of fresh LB at 37°C and were then passaged again (1:25) at mid-exponential phase (OD at 600 nm [OD<sub>600</sub>], 0.2) into fresh LB (28.8 ml) at 37°C. At an OD<sub>600</sub> of 0.2, sodium azide (200 mM) or sodium chloride (5 M NaCl) was added to a final concentration of 2 mM or 0.3 M NaCl, respectively. (E)-N-(4-fluorophenyl)-2-phenylethanesulfonamide (FPSS; Enamine Ltd., Kiev, Ukraine) (11) stock solutions (10 mM) were diluted in dimethyl sulfoxide (DMSO; Sigma-Aldrich, St. Louis, MO) and were filtered with 0.2-µm nylon membrane syringe filters (Acrodisc; Pall, Port Washington, NY). FPSS was added to a final concentration of 64 µM, except where noted

differently. For cold growth experiments, exponential-phase cultures that had been grown in LB at 37°C were moved to 16°C with shaking (225 rpm) immediately following the addition of either FPSS or an equal volume of DMSO. Phosphate limitation experiments were conducted in a synthetic medium (20). A low-phosphate (0.15 mM) synthetic medium (28.8 ml) was inoculated with 1.2 ml of culture (1:25) that had been grown in the same medium overnight at 37°C with shaking. At an OD<sub>600</sub> of 0.2, FPSS or an equal volume of DMSO was added, and samples were removed at regular intervals for β-galactosidase activity assays performed using cell permeabilization with chloroform as described by Kenney and Moran (38). OD<sub>600</sub> values of cell suspensions were used to calculate Miller units, while the protein concentration, determined by the Bradford assay (Bio-Rad, Hercules, CA), was used to calculate the specific activity of β-galactosidase, defined as the change in A<sub>420</sub> min<sup>-1</sup> mg of protein<sup>-1</sup>. At least two biological replicates were performed for each experiment.

***In vitro* transcription assays.** The phenol-chloroform-purified PCR product (amplified using primers DR1 and DR2 and plasmid pDLR1) was used as a DNA template for *in vitro* transcription assays. *In vitro* transcription that is initiated from the SigA2- and SigB-dependent promoters of the *L. monocytogenes fri* promoter generates RNA fragments of 185 and 120 bp, respectively. Reaction mixtures (40 µl) containing an *in vitro* transcription buffer (10 mM Tris-HCl [pH 7.8], 10 mM MgCl<sub>2</sub>, 0.5 mM EDTA, 1 mM DTT, 7.5 mM KCl, and 10 µg/ml acetylated bovine serum albumin [BSA]), His<sub>6</sub>-SigA or His<sub>6</sub>-SigB, and FPSS or DMSO were incubated at room temperature for 5 min. Purified *B. subtilis* RNA polymerase was added to the mixtures for a final protein concentration of 150 nM. The PCR product (330 ng) was added, followed by incubation at 37°C for 10 min. Transcription reactions were started by adding a mixture of nucleoside triphosphates (NTPs) (approximately 0.2 mM [final concentration] each ATP, CTP, GTP, and UTP and 1.7 nmol [α-<sup>32</sup>P]UTP [6,000 Ci mmol<sup>-1</sup>]) and incubating at 37°C for 10 min. Reactions were stopped by adding 60 µl of stop solution (0.5 M sodium acetate, 17 mM EDTA). RNA was precipitated by adding 330 µl ethanol (EtOH) and 2 µl glycogen (GlycoBlue; Invitrogen, Carlsbad, CA), followed by overnight storage at -20°C. RNA was collected by centrifugation (16,000 × g, 10 min, room temperature), washed with 70% EtOH, and resuspended in formamide loading dye. Samples were heated at 95°C for 5 min and were loaded onto a 6% Tris-borate-EDTA (TBE)-urea gel for separation. Transcripts were visualized using phosphorimaging.

**IEF and immunostaining.** Aliquots (15 ml) of mid-exponential-phase (OD<sub>600</sub>, 0.3) cells grown in LB at 37°C with shaking were harvested before and after the addition of FPSS (final concentration, 64 µM) or an equal volume of DMSO, at designated time points. Cells were centrifuged (6,000 × g, 3 min, 4°C), and pellets were resuspended in lysis buffer (100 mM Tris-HCl [pH 7.5], 1 mM EDTA, 1 mM phenylmethylsulfonyl fluoride [PMSF], 10 mM NaF). Cells were mechanically lysed using a bead-beater (Mini-Beadbeater-8; Biospec) for 3 min. Lysates were centrifuged (16,000 × g, 10 min, 4°C), and proteins were precipitated from the supernatant with ethanol. Protein pellets were resuspended in Novex isoelectric focusing (IEF) sample buffer (pH 3 to 7; Invitrogen) and were quantified

by a Bradford assay (Bio-Rad). Equivalent amounts of protein (40  $\mu$ g) were loaded onto an IEF minigel (Novex pH 3–7 IEF gel; Invitrogen) and were run according to the manufacturer's instructions. Proteins from gels were transferred to nitrocellulose membranes (0.2  $\mu$ m) in Towbin buffer (25 mM Tris-HCl [pH 8.3], 192 mM glycine) containing 20% (vol/vol) methanol. Bound proteins were probed with monoclonal anti-RsbV antibodies (39), provided by W. G. Haldenwang (University of Texas Health Science Center at San Antonio), and an alkaline phosphatase-conjugated anti-mouse secondary antibody (Invitrogen) and were visualized with the chromogenic substrate NBT (nitroblue tetrazolium)-BCIP (5-bromo-4-chloro-3-indolylphosphate) (Invitrogen).

**RNA extraction, cDNA synthesis, and quantitative reverse transcription-PCR (qRT-PCR).** *L. monocytogenes* strain 10403S  $\Delta sigB$  was streaked from frozen stocks onto brain heart infusion (BHI) agar plates and was incubated overnight at 37°C. An isolated colony was used to inoculate 5 ml BHI broth, which was incubated at 37°C overnight with shaking (225 rpm). A 50- $\mu$ l aliquot was transferred from this culture to 5 ml fresh, prewarmed BHI (1:100) and was grown to an OD<sub>600</sub> of 0.4. A 300- $\mu$ l aliquot was transferred to two Nephelo flasks containing 300 ml prewarmed BHI and was grown to an OD<sub>600</sub> of 0.4. An aliquot (5 ml) was removed from each culture and was added to 5 ml RNeasy Protect (Qiagen) to stop transcription. To the remaining cultures, 64  $\mu$ M FPSS or an equal volume of DMSO was added, and the flasks were returned to the incubator. After 15 min, another 5 ml was removed and treated as described above. Salt (final concentration, 0.3 M NaCl) was added to the cultures, and the cultures were returned to the incubator. After 15 min, a final 5-ml aliquot was removed and was treated as described above. Cells were pelleted (3,600  $\times$  g, 10 min, 4°C) after 5 min at room temperature in RNeasy Protect. Pellets were kept on ice until RNA extraction, which was performed as described previously (40). cDNA was synthesized as described elsewhere (41). TaqMan qPCR was performed on 10<sup>-1</sup>, 10<sup>-2</sup>, and 10<sup>-3</sup> dilutions of cDNA by using *sigB* and *rpoB* (36) primers and probes. A standard curve was generated using genomic chromosomal DNA isolated from *L. monocytogenes* 10403S. Copy numbers of *sigB* transcript levels were calculated from standard curves and were normalized to *rpoB* transcript levels, as described by Sue et al. (42).

**Statistical analysis.** Statistical analysis of *sigB* transcript levels from three biological replicates was performed using Student *t* tests at each time point with a statistical significance (*P*) value of <0.05 (JMP 9.0; SAS, Inc., Cary, NC).

## RESULTS AND DISCUSSION

In previous work, we showed that FPSS, a small molecule initially identified through high-throughput screening as an *L. monocytogenes*  $\sigma^B$  inhibitor, inhibited *B. subtilis*  $\sigma^B$  activity induced by salt exposure (0.3 M NaCl) (11), as monitored by a well-characterized  $\sigma^B$ -dependent single-copy *ctc-lacZ* transcriptional fusion (30). Here we aimed to define the molecular mechanism through which FPSS inhibits  $\sigma^B$  activity. We hypothesized that FPSS could inhibit  $\sigma^B$  activity by blocking the transcription of the gene encoding the sigma factor; therefore, we investigated the question of whether FPSS prevents the transcription of *sigB* in *L. monocytogenes*. We measured *sigB* transcript levels in *L. monocytogenes* 10403S  $\Delta sigB$  with *sigB* TaqMan qRT-PCR primers and a probe that can detect a signal in the null mutant due to the residual  $\sim$ 200 bp of the 5' end of the gene (34). The use of the  $\Delta sigB$  strain allowed us to monitor *sigB* transcript levels in response to FPSS addition in the presence of an environmental stress but in the absence of positive upregulation by the autoregulatory feedback loop formed by a second  $\sigma^B$ -dependent promoter located upstream of *rsbV*.

Treatment with FPSS did not significantly (*P*, >0.05 by the *t* test) reduce *sigB* mRNA transcript levels in *L. monocytogenes* before or after exposure to 0.3 M NaCl from those in DMSO-treated

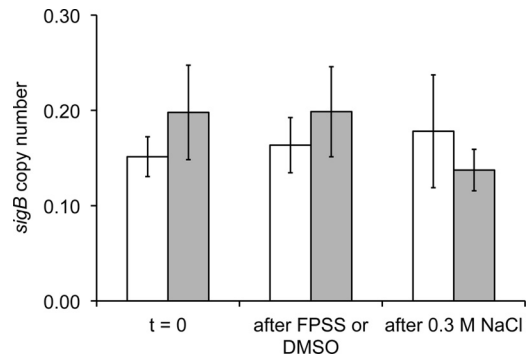


**FIG 2** *sigB* transcript copy numbers after addition of FPSS or DMSO. *L. monocytogenes* 10403S  $\Delta sigB$  was grown in BHI at 37°C with shaking (225 rpm). At an OD<sub>600</sub> of 0.4, 5 ml of culture was removed and was added to 5 ml RNeasy Protect (Qiagen) to stop transcription prior to RNA isolation (*t* = 0). FPSS (64  $\mu$ M) or an equal volume of DMSO was added to the remaining cultures. After 15 min, another 5-ml aliquot was removed for RNA isolation (“after FPSS or DMSO”). Salt (0.3 M [final concentration] NaCl) was added to both cultures, and after 15 min, another 5 ml of culture was collected (“after 0.3 M NaCl”). Mean values for *sigB* transcript copy numbers (in arbitrary units) from a DMSO-treated culture (open bars) and an FPSS-treated culture (shaded bars), calculated from three biological replicates, are shown with standard deviations. *sigB* transcript copy numbers were normalized to *rpoB* transcript copy numbers in order to calculate relative transcript levels.

control cultures (Fig. 2). These findings indicate that FPSS does not appear to operate at a transcriptional level to inhibit  $\sigma^B$  activity during mid-exponential-phase growth or in response to a sudden environmental stress.

**FPSS prevents  $\sigma^B$  activity in response to environmental stress, energy stress, and growth at low temperatures in *B. subtilis*.** Because we saw no transcriptional effect of FPSS in *L. monocytogenes*, we hypothesized that the molecule operates posttranslationally to inhibit  $\sigma^B$  activity. Therefore, to determine the effects of FPSS on  $\sigma^B$  activity, we chose to perform genetic experiments in *B. subtilis*, in which the  $\sigma^B$  signal transduction cascade has been well characterized. Initial sporulation experiments showed that addition of FPSS to mid-exponential-phase cultures of strain PB198 and the  $\Delta sigB$  mutant strain PB345 failed to alter sporulation significantly (data not shown) in either strain. We therefore concluded that FPSS specifically targets the signaling pathway that regulates  $\sigma^B$  rather than interfering more globally with other homologous partner-switching systems (e.g., SpoIIAB and SpoIIAA) (43, 44).

Energy and environmental stresses induce  $\sigma^B$  activity through two distinct pathways in *B. subtilis*. The response to energy stresses requires the phosphatase RsbP to dephosphorylate RsbV-P (16, 20, 22). An *rsbP*-null strain demonstrates normal  $\sigma^B$  activity in response to high-salt and ethanol exposure (22), indicating that RsbP is not an essential regulatory protein for the induction of  $\sigma^B$  activity in response to environmental stress. Therefore, to determine whether FPSS interacts with a member of the stressosome or the phosphatase RsbU, we investigated whether FPSS prevents the induction of  $\sigma^B$  activity in response to energy stresses. We hypothesized that if FPSS interferes solely with the environmental stress pathway, then the response to energy stress should be unaffected. We assayed three energy stress conditions in *B. subtilis*: entry into stationary phase, phosphate limitation, and azide stress.

The presence of FPSS at 64  $\mu$ M, a concentration previously shown to inhibit  $\sigma^B$  activity (11), prevented  $\sigma^B$  activity during

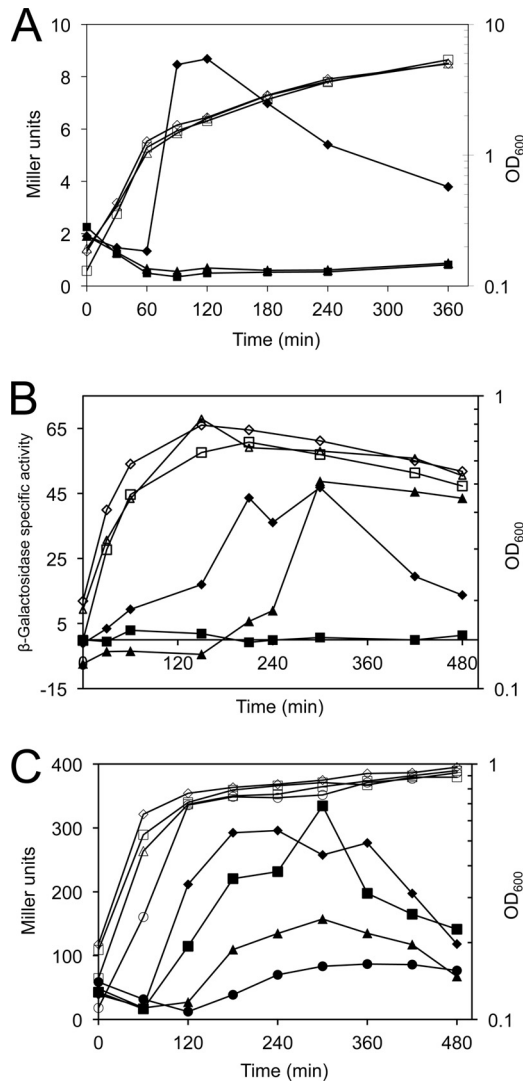


**FIG 3** Effect of FPSS on  $\sigma^B$  activity during energy stress.  $\beta$ -Galactosidase activity (filled symbols) and cell growth, measured by the  $OD_{600}$  (open symbols), from one representative experiment are shown. (A) Entry into stationary phase. Strains PB198 (*amyE::ctc-lacZ trpC2*) and PB345 (*amyE::ctc-lacZ trpC2 sigBA3::spc trpC2*) were grown in LB at 37°C with shaking (225 rpm). At mid-exponential phase ( $OD_{600}$  0.2), a sample of culture was removed, and 64  $\mu$ M FPSS (triangles) or an equal volume of DMSO (diamonds) was added to PB198, while PB345 was treated with DMSO (squares). (B) Azide stress. Strains PB198 and PB345 were grown in LB at 37°C with shaking (225 rpm) to mid-exponential phase. At an  $OD_{600}$  of 0.2 (time zero), cultures were treated with sodium azide (final concentration, 2 mM) and either 64  $\mu$ M FPSS (PB198) (triangles) or an equal volume of DMSO (diamonds) [PB198] or squares [PB345]. (C) Phosphate limitation. Strain PB198 was grown at 37°C with shaking (225 rpm) in a low-phosphate (15  $\mu$ M) defined medium with FPSS at 32  $\mu$ M (squares), 64  $\mu$ M (triangles), or 128  $\mu$ M (circles), or with a volume of DMSO equal to the volume of FPSS added to the culture treated with 128  $\mu$ M FPSS (diamonds).

entry into stationary phase (Fig. 3A) in PB198 cells grown at 37°C in LB, an effect that lasted for at least 5 h after entry into stationary phase, in contrast to the results for control cells treated with DMSO. Furthermore, FPSS delayed  $\sigma^B$  activity in response to sodium azide (2 mM), an inhibitor of ATP synthesis (Fig. 3B). The FPSS-treated culture showed induction of  $\sigma^B$  activity about 4 h after induction in the DMSO-treated culture, despite concurrent

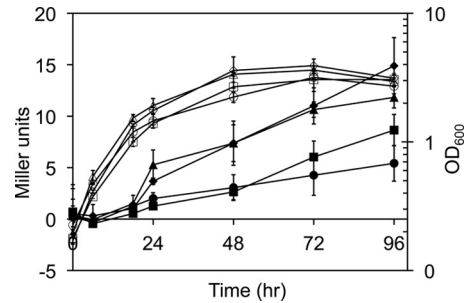


**FIG 4** Effect of FPSS on  $\sigma^B$  activation by growth at 16°C. Mean Miller units (filled symbols) and cell growth, monitored by the  $OD_{600}$  (open symbols), for two biological replicates are shown. Error bars, standard deviations. Strains PB198 (*amyE::ctc-lacZ trpC2*) and PB206 (*rsbV $\Delta$ 1 amyE::pDH32-ctc*) were grown at 37°C with shaking (225 rpm) in LB to mid-exponential phase ( $OD_{600}$  0.2). The strains were treated with 64  $\mu$ M FPSS or an equal volume of DMSO and were then transferred to 16°C with shaking (225 rpm). Results for PB198 treated with DMSO (diamonds) or 64  $\mu$ M FPSS (squares) and for PB206 treated with DMSO (triangles) or 64  $\mu$ M FPSS (circles) are shown.

cessation of growth in the two cultures. Finally, we grew strain PB198 in synthetic medium with limited phosphate (15  $\mu$ M) to induce phosphate starvation, and we treated parallel cultures with 0, 32, 64, or 128  $\mu$ M FPSS. We observed a delay in  $\sigma^B$  activity in cultures treated with FPSS, as well as decreased activity dependent on the concentration of FPSS added to the cultures (Fig. 3C). The addition of 64  $\mu$ M or 128  $\mu$ M FPSS resulted in  $\sim$ 46% or  $\sim$ 24% of the activity of the wild type, respectively. The perturbation of  $\sigma^B$  activity in response to both environmental and energy stresses suggests that FPSS does not interfere only with the function of the positive regulator RsbU or upstream members of the stressosome, which are not required for the response to energy stress (16), or only with RsbP or RsbQ, which are not required for  $\sigma^B$  activity in response to salt stress (22).

**FPSS inhibits  $\sigma^B$  chill induction independently of RsbV.** Another type of stress, growth at a low (16°C) temperature, induces  $\sigma^B$  activity in *B. subtilis*. Interestingly, the gradual induction of  $\sigma^B$  activity observed under these conditions occurs independently of the RsbT/RsbU/RsbV pathway in *B. subtilis* (23), indicating that induction of  $\sigma^B$  activity under these conditions does not depend on the phosphorylation state of RsbV. To determine whether FPSS prevents the induction of  $\sigma^B$  by interaction with RsbV or is dependent on the phosphorylation state of RsbV, we tested whether FPSS could prevent “chill induction” of  $\sigma^B$  activity. If FPSS interacts with RsbV to disrupt the release of  $\sigma^B$  from RsbW, we would expect to see no effect of FPSS on  $\sigma^B$  activity during growth at 16°C. Conversely, if FPSS interacts in an RsbV-independent manner, we would expect to see inhibition of  $\sigma^B$  activity in a  $\Delta$ *rsbV* mutant during cold growth. We grew *B. subtilis* PB198 and the  $\Delta$ *rsbV* strain PB206 (30) at 37°C in LB, treated the cells with FPSS or DMSO, shifted them to 16°C, and monitored  $\sigma^B$  activity (Fig. 4). DMSO-treated PB198 and PB206 showed induction of  $\sigma^B$  activity approximately 18 h after a shift to 16°C, compared to cultures treated with 64  $\mu$ M FPSS prior to the temperature shift. The inhibition of  $\sigma^B$  activity by FPSS in a *B. subtilis* strain lacking *rsbV* suggests that FPSS acts via at least one mechanism that is independent of RsbV and independent of either the RsbU or the RsbP phosphatase.

**FPSS prevents  $\sigma^B$  activation.** Having determined that FPSS prevents  $\sigma^B$  activity in response to the three known categories of

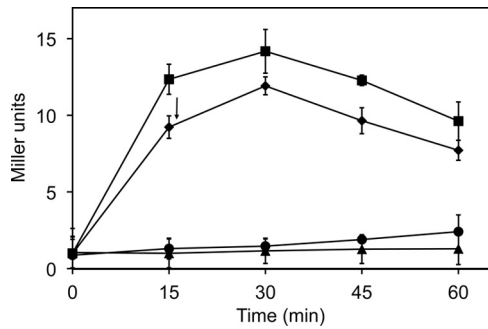


**FIG 5** Effect of delayed addition of FPSS on salt-induced  $\sigma^B$  activity. At mid-exponential phase ( $OD_{600}$ , 0.2), PB198 (*amyE::ctc-lacZ trpC2*) grown in LB at 37°C with shaking (225 rpm) was treated with either H<sub>2</sub>O and DMSO (●), 0.3 M NaCl and DMSO (■), 0.3 M NaCl and 64  $\mu$ M FPSS (▲), or 0.3 M NaCl, with 64  $\mu$ M FPSS added after 15 min of sampling (indicated by an arrow) (◆). Mean  $\beta$ -galactosidase activity for two biological replicates is shown. Error bars, standard deviations.

stress in *B. subtilis*, we asked: does FPSS prevent  $\sigma^B$  activity by altering the activation of  $\sigma^B$  (meaning its switch from an inactive, bound state to its free, active state) or, rather, does it inhibit the activity of the sigma factor, i.e., its transcriptional function once  $\sigma^B$  is released from its antagonist, RsbW? To address this question, we measured the effect of adding FPSS 15 min after the induction of  $\sigma^B$  activity by salt stress (0.3 M NaCl). We hypothesized that if FPSS affects either the activation of  $\sigma^B$  or the recruitment of the RNAP holoenzyme to  $\sigma^B$ -dependent promoter sites, the addition of FPSS after the induction of  $\sigma^B$  activity should not affect the development of  $\sigma^B$  activity in response to an environmental stress. We observed a level of accumulation of the  $\beta$ -galactosidase enzyme in cultures treated with FPSS after exposure to salt similar to that in control cultures treated with DMSO (Fig. 5). In agreement with our previous work, we saw no  $\sigma^B$  activity in cultures treated with FPSS prior to the addition of salt. The absence of an effect on  $\sigma^B$  activity after  $\sigma^B$  activity had been induced suggests that FPSS inhibits the activation of  $\sigma^B$  rather than interfering with  $\sigma^B$ -dependent transcription once  $\sigma^B$  is active and is promoting transcription from  $\sigma^B$ -dependent binding sites.

**FPSS does not inhibit  $\sigma^B$  transcription activity *in vivo* and *in vitro*.** To further investigate the ability of FPSS to inhibit  $\sigma^B$  activity, we used genetic experiments to investigate the effect of FPSS on the transcriptional role of  $\sigma^B$  as an RNAP subunit. In *B. subtilis* and *L. monocytogenes*, the gene encoding  $\sigma^B$  lies within an eight-gene operon ( $P_A$ -*rsbR*-*rsbS*-*rsbT*-*rsbU*- $P_B$ -*rsbV*-*rsbW*-*sigB*-*rsbX*) known as the *sigB* operon (45, 46). A  $\sigma^B$ -dependent promoter lies upstream of *sigB*, creating an autoregulatory feedback loop after  $\sigma^B$  becomes active. We used *B. subtilis* strain PB213 (30), which contains an inducible promoter upstream of *rsbV*, to enable IPTG-induced expression of  $\sigma^B$ . The addition of IPTG to PB213 induces  $\sigma^B$  activity, as measured by a  $\sigma^B$ -dependent reporter fusion, in this *rsbW*-null mutant (30), presumably by increasing the amount of active, unbound  $\sigma^B$  in the absence of the anti-sigma factor antagonist.

As shown in Fig. 6,  $\sigma^B$  activity in strain PB213 was rapidly induced upon addition of IPTG, even when 64  $\mu$ M FPSS was added immediately before the addition of IPTG. This result, again, suggests that FPSS has no effect on the transcriptional function of

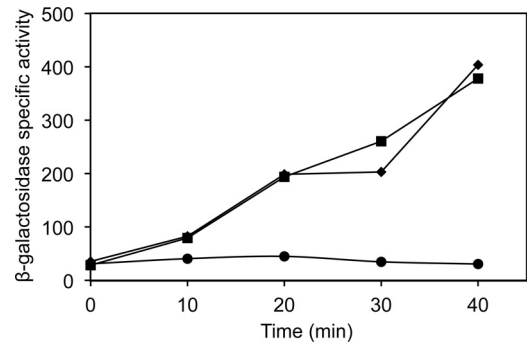


**FIG 6** Effect of FPSS on  $\sigma^B$  activity by artificial induction. PB213 [ $P_{spac}$  (*rsbV*<sup>+</sup> *rsbW* $\Delta$ 1 *sigB*<sup>+</sup> *rsbX*<sup>+</sup>) *amyE::pDH32-ctc trpC2*] was grown in BLB at 37°C with shaking (225 rpm). At an  $OD_{600}$  of 0.4 (time zero), 64  $\mu$ M FPSS or DMSO and IPTG (final concentration, 1 mM) or distilled H<sub>2</sub>O were added.  $\beta$ -Galactosidase activities were determined for PB213 with H<sub>2</sub>O and DMSO (●), IPTG and DMSO (■), and IPTG and FPSS (◆). Results from a representative experiment are shown.

$\sigma^B$  once  $\sigma^B$  has become active. These results provide additional evidence to support our hypothesis that FPSS interferes with the regulation of  $\sigma^B$  rather than with its role in transcription initiation.

We next sought to rule out the possibility that FPSS binds directly to  $\sigma^B$  by using *in vitro* transcription assays. If FPSS binds directly to  $\sigma^B$ , it might interfere either with the sigma factor's ability to bind to RNAP or with its release from RsbW. We performed transcription assays in a simplified *in vitro* system containing *B. subtilis* RNAP, His<sub>6</sub>-tagged *L. monocytogenes*  $\sigma^B$  or  $\sigma^A$  (as a control), and a fragment of the *L. monocytogenes* *fri* promoter region containing one  $\sigma^B$ - and one  $\sigma^A$ -dependent promoter site (37).

The reconstituted holoenzymes were successfully transcribed from both *L. monocytogenes* promoter sites (Fig. 7). Control reactions without any added sigma factors showed that residual *B. subtilis*  $\sigma^A$  contained in the purified RNAP protein fraction initiated transcription from the *L. monocytogenes*  $\sigma^A$ -dependent promoter site (Fig. 7, lane 11), but the addition of exogenous, purified *L. monocytogenes*  $\sigma^A$  and  $\sigma^B$  promoted higher transcript levels from the template's  $\sigma^A$ - and  $\sigma^B$ -dependent promoter sites (lanes 13 and 12, respectively). DMSO addition did not affect the abilities of  $\sigma^A$  and  $\sigma^B$  to drive transcription from either promoter (Fig. 7, lanes 14 and 15). We performed two titration experiments to test the effect of FPSS on transcription from a  $\sigma^B$ -dependent promoter site. In the first titration experiment, increasing amounts of  $\sigma^B$  added to reaction mixtures caused higher levels of transcripts to be produced from the  $\sigma^B$  promoter (Fig. 7, lanes 1 to 5). Transcription in these reactions from the  $\sigma^B$ -dependent promoter site was uninhibited by the presence of FPSS up to ~1,000-fold the concentration of  $\sigma^B$  and *B. subtilis* RNAP (Fig. 7, lanes 6 to 10). In the second experiment, titration with increasing amounts of FPSS (up to 1,000-fold higher) relative to  $\sigma^B$  (Fig. 7, lanes 17 to 21) did not inhibit transcription relative to that in a control reaction mixture containing DMSO (lane 16). Since the RNAP- $\sigma^B$  holoenzyme was able to transcribe from a  $\sigma^B$ -dependent promoter despite the presence of a relatively high concentration of FPSS, these data provide additional support for the idea that *in vitro*, FPSS does not prevent the binding of  $\sigma^B$  to core RNAP and does not prevent the recognition of  $\sigma^B$ -dependent promoter sites.

**FPSS inhibits  $\sigma^B$  activity specifically, likely by preventing RsbW- $\sigma^B$  partner switching.** The discovery that FPSS inhibits the

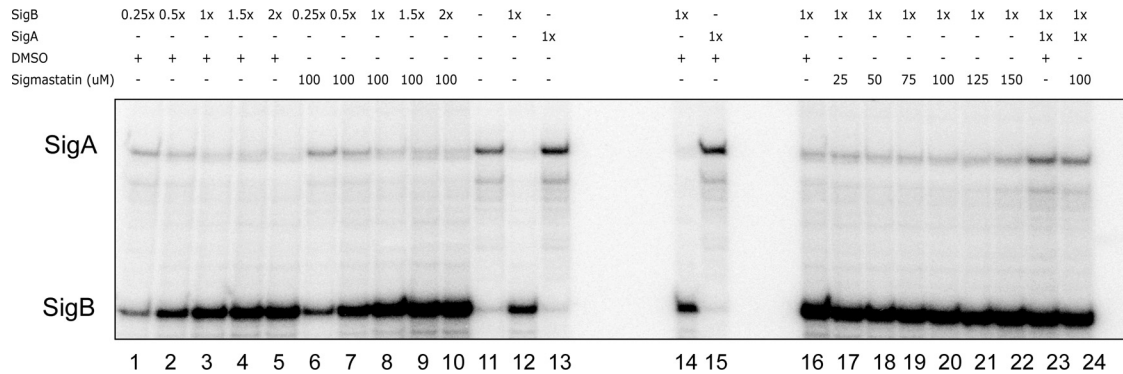


**FIG 7** Effect of FPSS on *in vitro* transcription of the *L. monocytogenes*  $\sigma^B$ -dependent promoter. (Left lanes) *B. subtilis* RNAP (150 nM) was added to reaction mixtures containing various concentrations of  $\sigma^B$  (37.5, 75, 150, 225, or 300 nM) in the presence of DMSO (lanes 1 to 5) or 100  $\mu$ M FPSS (lanes 6 to 10). Control reactions (lanes 12 and 13) exhibit sigma factor-initiated transcription from both promoters, even in the presence of DMSO (lanes 14 and 15). (Right lanes) *B. subtilis* RNAP (150 nM) was added to reaction mixtures containing  $\sigma^B$  (150 nM) in the presence of DMSO (lane 16) or various concentrations of FPSS (25, 50, 75, 100, 125, or 150  $\mu$ M) (lanes 17 to 22).

activation of  $\sigma^B$  led us to investigate potential targets to which it might bind as a mechanism for its inhibitory activity. We speculated that since FPSS does not appear to interact with either the RsbU or the RsbP phosphatase alone, it might interfere with the partner-switching module RsbV-RsbW- $\sigma^B$ , a shared component of both pathways that plays a central role in regulating  $\sigma^B$ . To test that hypothesis, we explored the phosphorylation state of RsbV in response to environmental stress in the presence of FPSS. Isoelectric focusing and immunostaining of RsbV, used to separate the unphosphorylated and phosphorylated forms of RsbV, revealed that FPSS prevents the *in vivo* dephosphorylation of RsbV-P in *B. subtilis* in response to salt stress (Fig. 8). The dephosphorylation of RsbV-P is a crucial step necessary for freeing and activating  $\sigma^B$  upon stress signaling. These results suggest that FPSS disrupts the ability of RsbV to switch partners with  $\sigma^B$ , thus leaving  $\sigma^B$  bound to RsbW and hence inactive.

Central to the regulation of  $\sigma^B$  in response to energy and sudden environmental stress in *B. subtilis* is the dephosphorylation of the anti-anti-sigma factor RsbV, a member of the partner-switching module directly responsible for controlling the free or RsbW-bound state of  $\sigma^B$  (30, 39, 47). RsbW has a higher affinity for unphosphorylated RsbV than for  $\sigma^B$  (48), but the kinase function of RsbW keeps a majority of RsbV phosphorylated at baseline expression levels of the *sigB* operon in unstressed cells, and thus, RsbW remains bound to  $\sigma^B$  (49). The phosphatases RsbU and RsbP dephosphorylate RsbV-P and modulate  $\sigma^B$  activity in a

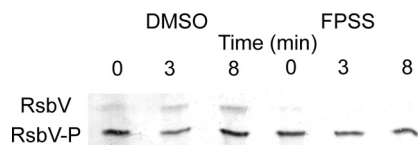


**FIG 8** IEF analysis of phosphorylation of *B. subtilis* RsbV after exposure to salt stress. *B. subtilis* PB2 was grown in LB at 37°C with shaking (225 rpm) to the mid-exponential phase ( $OD_{600}$ , 0.3) and was treated with 64  $\mu$ M FPSS or an equivalent volume of DMSO. Cultures were then treated with 0.3 M (final concentration) NaCl and were incubated at 37°C with shaking. Samples were removed before (0 min) and after (3 and 8 min) salt treatment. Crude extracts (40  $\mu$ g protein) were separated using vertical IEF, transferred to nitrocellulose membranes, and probed using a monoclonal anti-RsbV antibody.

tightly controlled circuit, countering the antagonistic role of RsbW (49). In *B. subtilis*, RsbU and RsbP function independently, responding to separate stress-sensing components. Our finding that the response to stress controlled by both pathways possessing these phosphatases is inhibited by FPSS allows us to conclude that neither RsbU nor RsbP is the exclusive target of FPSS and that FPSS interacts with a component shared by both stress activation pathways.

Our analysis of the phosphorylation state of RsbV in *B. subtilis* exposed to salt stress indicates that FPSS prevents the dephosphorylation of RsbV that is seen in untreated control cells in response to the stress. The sum of our findings, namely, (i) that RsbV is not necessary for inhibition by FPSS and (ii) that dephosphorylation of RsbV does not appear to occur in FPSS-treated cells in response to stress, leads us to hypothesize that the likely target of FPSS is RsbW. We speculate that FPSS may act to prevent the release of RsbW from  $\sigma^B$ , by binding either to RsbW alone or to the interface of the proteins. Additional biochemical experiments are needed to determine the precise molecular mechanism of the inhibitory action of FPSS on the RsbW and  $\sigma^B$  components of the partner-switching module that plays a central role in regulating  $\sigma^B$  activity.

Novel inhibitors of  $\sigma^B$  in *B. subtilis* and *L. monocytogenes* may inhibit homologous sigma factors in other organisms, such as *S. aureus*, and such inhibitors could offer novel therapeutic approaches as alternatives to broad-spectrum antibiotics. Identification of the mechanism of FPSS for inhibiting  $\sigma^B$  activity will improve our understanding of how  $\sigma^B$  activity is regulated in *B. subtilis* and *L. monocytogenes*, and how similar, homologous systems are regulated in other Gram-positive organisms with similar regulatory elements.

#### ACKNOWLEDGMENTS

The work was supported by National Institutes of Health awards 5R01AI052151-09 (to K.J.B.) and GM-047446 (to J.D.H.). Support for student training was provided by USDA National Needs Graduate Fellowship Competitive Grant 2007-38420-17751 from the National Institute of Food and Agriculture.

The contents of the article are solely the responsibility of the authors and do not necessarily represent the official views of the NIH.

## REFERENCES

1. Ferreira A, Gray M, Wiedmann M, Boor KJ. 2004. Comparative genomic analysis of the *sigB* operon in *Listeria monocytogenes* and in other Gram-positive bacteria. *Curr. Microbiol.* 48:39–46.
2. Oliver H, Orsi R, Ponnala L, Keich U, Wang W, Sun Q, Cartinhour S, Filiatrault M, Wiedmann M, Boor KJ. 2009. Deep RNA sequencing of *L. monocytogenes* reveals overlapping and extensive stationary phase and sigma B-dependent transcriptomes, including multiple highly transcribed noncoding RNAs. *BMC Genomics* 10:641. doi:10.1186/1471-2164-10-641.
3. Raengpradub S, Wiedmann M, Boor KJ. 2008. Comparative analysis of the  $\sigma^B$ -dependent stress responses in *Listeria monocytogenes* and *Listeria innocua* strains exposed to selected stress conditions. *Appl. Environ. Microbiol.* 74:158–171.
4. Nannapaneni P, Hertwig F, Depke M, Hecker M, Mäder U, Völker U, Steil L, van Hijum SAFT. 2012. Defining the structure of the general stress regulon of *Bacillus subtilis* using targeted microarray analysis and random forest classification. *Microbiology* 158:696–707.
5. Price CW, Fawcett P, Ceremonie H, Su N, Murphy CK, Youngman P. 2001. Genome-wide analysis of the general stress response in *Bacillus subtilis*. *Mol. Microbiol.* 41:757–774.
6. Ollinger J, Bowen B, Wiedmann M, Boor KJ, Bergholz TM. 2009. *Listeria monocytogenes*  $\sigma^B$  modulates PrfA-mediated virulence factor expression. *Infect. Immun.* 77:2113–2124.
7. Nadon CA, Bowen BM, Wiedmann M, Boor KJ. 2002. Sigma B contributes to PrfA-mediated virulence in *Listeria monocytogenes*. *Infect. Immun.* 70:3948–3952.
8. Fouet A, Namy O, Lambert G. 2000. Characterization of the operon encoding the alternative sigma B factor from *Bacillus anthracis* and its role in virulence. *J. Bacteriol.* 182:5036–5045.
9. Bischoff M, Dunman P, Kormanec J, Macapagal D, Murphy E, Mounts W, Berger-Bachi B, Projan S. 2004. Microarray-based analysis of the *Staphylococcus aureus*  $\sigma^B$  regulon. *J. Bacteriol.* 186:4085–4099.
10. Horsburgh MJ, Aish JL, White IJ, Shaw L, Lithgow JK, Foster SJ. 2002.  $\sigma^B$  modulates virulence determinant expression and stress resistance: characterization of a functional *rsbU* strain derived from *Staphylococcus aureus* 8325-4. *J. Bacteriol.* 184:5457–5467.
11. Palmer ME, Chaturongakul S, Wiedmann M, Boor KJ. 2011. The *Listeria monocytogenes*  $\sigma^B$  regulon and its virulence-associated functions are inhibited by a small molecule. *mBio* 2(6):e00241–11. doi:10.1128/mBio.00241-11.
12. Hecker M, Pané-Farré J, Völker U. 2007. SigB-dependent general stress response in *Bacillus subtilis* and related gram-positive bacteria. *Annu. Rev. Microbiol.* 61:215–236.
13. Marles-Wright J, Grant T, Delumeau O, van Duinen G, Firbank SJ, Lewis PJ, Murray JW, Newman JA, Quin MB, Race PR, Rohou A, Tichelaar W, van Heel M, Lewis RJ. 2008. Molecular architecture of the “stressosome,” a signal integration and transduction hub. *Science* 322:92–96.
14. Kim T-J, Gaidenko TA, Price CW. 2004. In vivo phosphorylation of partner switching regulators correlates with stress transmission in the environmental signaling pathway of *Bacillus subtilis*. *J. Bacteriol.* 186:6124–6132.
15. Delumeau O, Chen CC, Murray JW, Yudkin MD, Lewis RJ. 2006. High-molecular-weight complexes of RsbR and paralogues in the environmental signaling pathway of *Bacillus subtilis*. *J. Bacteriol.* 188:7885–7892.
16. Voelker U, Voelker A, Maul B, Hecker M, Dufour A, Haldenwang WG. 1995. Separate mechanisms activate sigma B of *Bacillus subtilis* in response to environmental and metabolic stresses. *J. Bacteriol.* 177:3771–3780.
17. Yang X, Kang CM, Brody MS, Price CW. 1996. Opposing pairs of serine protein kinases and phosphatases transmit signals of environmental stress to activate a bacterial transcription factor. *Genes Dev.* 10:2265–2275.
18. Gaidenko TA, Bie X, Baldwin EP, Price CW. 2011. Substitutions in the presumed sensing domain of the *Bacillus subtilis* stressosome affect its basal output but not response to environmental signals. *J. Bacteriol.* 193:3588–3597.
19. Eymann C, Schulz S, Gronau K, Becher D, Hecker M, Price CW. 2011. In vivo phosphorylation patterns of key stressosome proteins define a second feedback loop that limits activation of *Bacillus subtilis*  $\sigma^B$ . *Mol. Microbiol.* 80:798–810.
20. Zhang S, Haldenwang WG. 2005. Contributions of ATP, GTP, and redox state to nutritional stress activation of the *Bacillus subtilis*  $\sigma^B$  transcription factor. *J. Bacteriol.* 187:7554–7560.
21. Brody MS, Vijay K, Price CW. 2001. Catalytic function of an  $\alpha/\beta$  hydrolase is required for energy stress activation of the  $\sigma^B$  transcription factor in *Bacillus subtilis*. *J. Bacteriol.* 183:6422–6428.
22. Vijay K, Brody MS, Fredlund E, Price CW. 2000. A PP2C phosphatase containing a PAS domain is required to convey signals of energy stress to the  $\sigma^B$  transcription factor of *Bacillus subtilis*. *Mol. Microbiol.* 35:180–188.
23. Brigulla M, Hoffmann T, Krisp A, Volker A, Bremer E, Volker U. 2003. Chill induction of the SigB-dependent general stress response in *Bacillus subtilis* and its contribution to low-temperature adaptation. *J. Bacteriol.* 185:4305–4314.
24. Shin J-H, Brody MS, Price CW. 2010. Physical and antibiotic stresses require activation of the RsbU phosphatase to induce the general stress response in *Listeria monocytogenes*. *Microbiology* 156:2660–2669.
25. Chaturongakul S, Boor KJ. 2006.  $\sigma^B$  activation under environmental and energy stress conditions in *Listeria monocytogenes*. *Appl. Environ. Microbiol.* 72:5197–5203.
26. Chaturongakul S, Boor KJ. 2004. RsbT and RsbV contribute to  $\sigma^B$ -dependent survival under environmental, energy, and intracellular stress conditions in *Listeria monocytogenes*. *Appl. Environ. Microbiol.* 70:5349–5356.
27. Martinez L, Reeves A, Haldenwang W. 2010. Stressosomes formed in *Bacillus subtilis* from the RsbR protein of *Listeria monocytogenes* allow  $\sigma^B$  activation following exposure to either physical or nutritional stress. *J. Bacteriol.* 192:6279–6286.
28. Yanisch-Perron C, Vieira J, Messing J. 1985. Improved M13 phage cloning vectors and host strains: nucleotide sequences of the M13mp18 and pUC19 vectors. *Gene* 33:103–119.
29. Price CW, Doi RH. 1985. Genetic mapping of *rpoD* implicates the major sigma factor of *Bacillus subtilis* RNA polymerase in sporulation initiation. *Mol. Gen. Genet.* 201:88–95.
30. Boylan SA, Rutherford A, Thomas SM, Price CW. 1992. Activation of *Bacillus subtilis* transcription factor sigma B by a regulatory pathway responsive to stationary-phase signals. *J. Bacteriol.* 174:3695–3706.
31. Boylan SA, Redfield AR, Price CW. 1993. Transcription factor sigma B of *Bacillus subtilis* controls a large stationary-phase regulon. *J. Bacteriol.* 175:3957–3963.
32. Rauch M, Luo Q, Muller-Altrock S, Goebel W. 2005. SigB-dependent *in vitro* transcription of *prfA* and some newly identified genes of *Listeria monocytogenes* whose expression is affected by PrfA *in vivo*. *J. Bacteriol.* 187:800–804.
33. Bishop DK, Hinrichs DJ. 1987. Adoptive transfer of immunity to *Listeria monocytogenes*. The influence of *in vitro* stimulation on lymphocyte subset requirements. *J. Immunol.* 139:2005–2009.
34. Wiedmann M, Arvik TJ, Hurley RJ, Boor KJ. 1998. General stress transcription factor sigma B and its role in acid tolerance and virulence of *Listeria monocytogenes*. *J. Bacteriol.* 180:3650–3656.
35. Xue G-P, Johnson JS, Dalrymple BP. 1999. High osmolarity improves the electro-transformation efficiency of the gram-positive bacteria *Bacillus subtilis* and *Bacillus licheniformis*. *J. Microbiol. Methods* 34:183–191.
36. Bergholz TM, den Bakker HC, Fortes ED, Boor KJ, Wiedmann M. 2010. Salt stress phenotypes in *Listeria monocytogenes* vary by genetic lineage and temperature. *Foodborne Pathog. Dis.* 7:1537–1549.
37. Olsen KN, Larsen MH, Gahan CGM, Kallipolitis B, Wolf XA, Rea R, Hill C, Ingmer H. 2005. The Dps-like protein Fri of *Listeria monocytogenes* promotes stress tolerance and intracellular multiplication in macrophage-like cells. *Microbiology* 151:925–933.
38. Kenney TJ, Moran CP, Jr. 1987. Organization and regulation of an operon that encodes a sporulation-essential sigma factor in *Bacillus subtilis*. *J. Bacteriol.* 169:3329–3339.
39. Benson AK, Haldenwang WG. 1993. *Bacillus subtilis* sigma B is regulated by a binding protein (RsbW) that blocks its association with core RNA polymerase. *Proc. Natl. Acad. Sci. U. S. A.* 90:2330–2334.
40. Bergholz TM, Bowen B, Wiedmann M, Boor KJ. 2012. *Listeria monocytogenes* shows temperature-dependent and -independent responses to salt stress, including responses that induce cross-protection against other stresses. *Appl. Environ. Microbiol.* 78:2602–2612.
41. Oliver HF, Orsi RH, Wiedmann M, Boor KJ. 2010. *Listeria monocytogenes*  $\sigma^B$  has a small core regulon and a conserved role in virulence but makes differential contributions to stress tolerance across a diverse collection of strains. *Appl. Environ. Microbiol.* 76:4216–4232.
42. Sue D, Fink D, Wiedmann M, Boor KJ. 2004.  $\sigma^B$ -dependent gene induction and expression in *Listeria monocytogenes* during osmotic and



- acid stress conditions simulating the intestinal environment. *Microbiology* 150:3843–3855.
43. Alper S, Dufour A, Garsin DA, Duncan L, Losick R. 1996. Role of adenosine nucleotides in the regulation of a stress-response transcription factor in *Bacillus subtilis*. *J. Mol. Biol.* 260:165–177.
  44. Alper S, Duncan L, Losick R. 1994. An adenosine nucleotide switch controlling the activity of a cell type-specific transcription factor in *B. subtilis*. *Cell* 77:195–205.
  45. Kalman S, Duncan ML, Thomas SM, Price CW. 1990. Similar organization of the *sigB* and *spoIIA* operons encoding alternate sigma factors of *Bacillus subtilis* RNA polymerase. *J. Bacteriol.* 172:5575–5585.
  46. Wise AA, Price CW. 1995. Four additional genes in the *sigB* operon of *Bacillus subtilis* that control activity of the general stress factor sigma B in response to environmental signals. *J. Bacteriol.* 177:123–133.
  47. Benson AK, Haldenwang WG. 1993. Regulation of sigma B levels and activity in *Bacillus subtilis*. *J. Bacteriol.* 175:2347–2356.
  48. Delumeau O, Lewis RJ, Yudkin MD. 2002. Protein-protein interactions that regulate the energy stress activation of  $\sigma^B$  in *Bacillus subtilis*. *J. Bacteriol.* 184:5583–5589.
  49. Locke JCW, Young JW, Fontes M, Jiménez MJH, Elowitz MB. 2011. Stochastic pulse regulation in bacterial stress response. *Science* 334:366–369.